Progress In Electromagnetics Research, Vol. 147, 81–93, 2014

Challenges in Application of Luminescent Materials, a Tutorial Overview

Cees Ronda*

(*Invited Review*)

Abstract—In this paper, a number of different application fields of inorganic luminescent materials are being discussed. In a tutorial manner, it will be shown how device requirements are being translated into properties the luminescent materials need to have. To this end many different material properties that have a strong influence on the device performance are discussed, such as the shape, the spectral position of the absorption- and emission bands and the decay time of the emission. The light yield under excitation with ionizing radiation, the energy resolution and the occurrence of afterglow are being treated as well. Subsequently, strategies are shown how to optimize these properties. Examples are given for light sources (fluorescent lamps and LEDs), radiation sources used for disinfection purposes and also for devices used in medical imaging and in horticultural applications.

1. LUMINESCENT MATERIALS FOR LEDS

The first very successful electrical light source, the incandescent lamp, is around for about 150 years. Their widespread use was a revolution in view of ease of use and the absence of smell. They also played a major role in the electrification of many countries. Incandescent lamps are now gradually being phased out, in view of the rather low light generation efficiency of this lighting concept. The light generation efficiency is usually expressed in terms of lm/W, or in other words the amount of visible light generated divided by the electrical energy used to generate the light. The eye sensitivity for photons is strongly dependent on their wavelength. Incandescent lamps have an efficacy in the order of 10 lm/W. Higher filament temperatures result in higher efficacies, this is being applied in halogen lamps, with efficacies up to some 20 lm/W.

The next revolution in general lighting was marked by the invention of the fluorescent lamp. Important inventive steps were disclosed in [1], the first commercially viable product was invented by GE, in 1936 [2]. Initially, this concept was thought to be very suitable for colored advertisement lamps, especially blue light could be generated with much higher efficacy than by filtering blue light out of the light generated by incandescent lamps. Very soon afterwards, the potential of this concept to generate white light became very clear and already before the Second World War, fluorescent lamps were in use. Fluorescent lamps do not generate as much IR radiation as incandescent lamps, for this reason their efficacy is much higher than that of incandescent lamps. In the 1970-ies, after the invention of rare-earth based luminescent materials, a significant further increase in efficacy was realized. Again, the dependence of the eye-sensitivity on the photon wavelength played an important role. Most of the luminescent materials applied in fluorescent lamps before the advent of rare-earth phosphors show broad emission spectra, f.e., spectra with a FWHM of 50–100 nm. To generate white light with a high color rendering index (the ability to reproduce all colors in a natural way), blue, green and red light have to be present in the emission spectrum of the lamps, with maxima at about 450 nm, 550 nm and

Received 11 May 2014, Accepted 19 June 2014, Scheduled 23 June 2014
* Corresponding author: Cees Ronda (cees.ronda@philips.com).
The author is with the Philips Group Innovation Research, High Tech Campus 4, 5656 AE Eindhoven, The Netherlands.

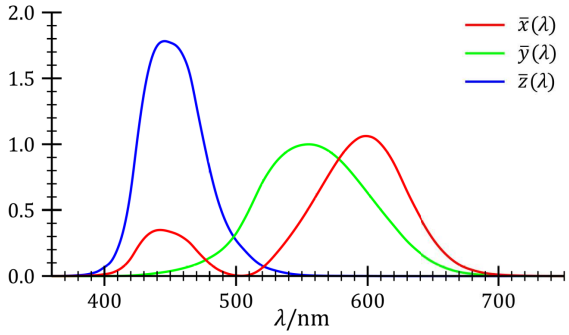

Figure 1. Chromatic eye response curves (taken from [3]).

600 nm, see Figure 1. In this figure, the CIE's (Commission Internationale de l'Eclairage) color matching functions are numerical descriptions of the chromatic response of the human eye; the green curve gives the overall eye sensitivity. Especially in the red part of the spectrum, the eye sensitivity decreases strongly above 600 nm and for this reason broad emission spectra in the red part of the spectrum lead to a significant loss in lumen output, even though the quantum efficiencies of the luminescent material applied to generate red light may be very high.

The material Y_2O_3:Eu (applied widely in fluorescent lamps) shows almost monochromatic emission at 610 nm, without a long tail in the extended red part of the visible spectrum. Nowadays fluorescent lamps can have efficacies of up to some 100 lm/W, i.e., 10 times higher than incandescent lamps. Despite this very significant increase in efficacy, the energy efficiency of fluorescent lamps is still rather low. This is due to the fact that the spectrum emitted by the low pressure Hg-discharge that is operating in fluorescent lamps consists mainly of photons with wavelength 185 nm and 254 nm. To generate visible light, these photons have to be downconverted to photons with significantly smaller photon energies. Together with the discharge efficiency of 70%, the resulting overall efficiency of fluorescent lamps is only some 25%. Compact fluorescent lamps have even lower efficiencies: 15%. Looking at the wavelengths, based on energy conservation it would be possible to generate two photons in the green and red part of the spectrum (or even one blue photon and a red photon) after absorption of one UV photon originating from the Hg-discharge (quantum cutting). Indeed, there has been extensive research into this direction. Systems have been found with quantum efficiencies clearly exceeding 100%, based on cascade emission on Pr^{3+} [4, 5] and also in ion pairs [6, 7]. In the case of Pr^{3+}, one of the photons generated has a wavelength of 408 nm, which is too short for high color rendering and attempts to transfer this energy to ions like Mn^{2+} or Cr^{3+} to obtain more useful photons have failed for reasons not understood yet. The other photon generated in the cascade has a wavelength of about 615 nm, i.e., very suitable for application in light sources with good color rendering and high lumen output.

The next revolution in lighting is now going on. Inorganic and organic LEDs, operated at low voltage generate light by recombination of electron and holes. We will now focus on the challenges in luminescent materials for application in inorganic LEDs.

In LED lamps, inorganic LEDs based on InGaN are used that emit light in the spectral range from near UV to blue. White light is generated by the application of one or more luminescent materials. One could also imagine a different concept: the use of LEDs emitting at different wavelengths to generate white light only, i.e., without phosphors. Intrinsically, this concept has the potential to have the highest energy efficiency, as each LED can be operated at the lowest possible operation voltage that matches the energy of the photons emitted. However, this approach suffers from the lack of an efficient green emitting LED and the fact that the red emitting LED shows a significant shift of the red emission band as a function of the temperature. When using a blue pump LED, the phosphor layer applied has to be at least partially transparent for blue light, in case of a UV LED, this is undesired: less visible light is generated and UV light is harmful, the harmfulness being dependent on the wavelength. The most frequently used concept of a blue LED combined with a yellow emitting phosphor suffers from too low a red light intensity, enabling only high color temperatures. This can be circumvented by adding a red emitting phosphor. In case of UV LEDs, also a blue emitting phosphor is needed. A graphical overview

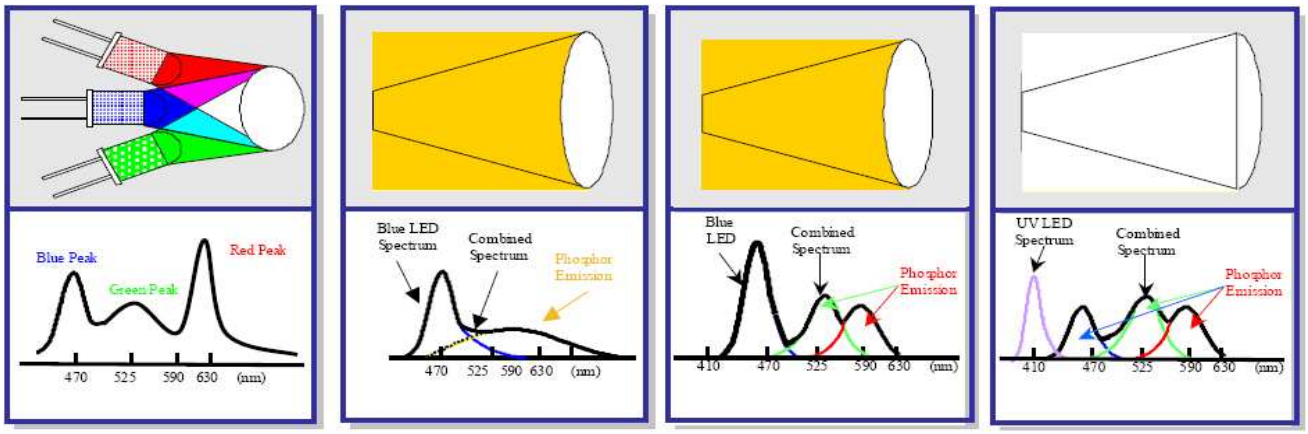

Figure 2. Concepts to create white light using LEDs.

is given in Figure 2.

The luminescent materials applied in LEDs have to fulfill a number of requirements, the most important ones are:

- Strong absorption of the LED emitting wavelength as at least a significant amount of the light emitted by the LED has to be absorbed, in case of UV emitting LEDs in principle even all UV radiation. It is also advantageous when the absorption transitions are broad, to at least partly compensate for small variations in LED emission wavelengths. As will elucidated further below, activator ions with strong optical transitions also show broad absorption bands, in this way effectively combining two important requirements.
- High quantum efficiency also at elevated temperatures and absence of saturation. The intensity of the radiation in LEDs is much higher than in fluorescent lamps (some 50 W/cm^2 vs. 0.05 W/cm^2) and consequently the phosphor layer in LEDs can reach temperatures well above 100 °C. The absence of saturation requires that the absorption strength and the emission decay time need to be balanced. This is especially important for Eu^{2+} phosphors in which the absorption strength is very high, even higher than in case of Ce^{3+} (many overlapping excited states), whereas the decay time is relatively large, in the order of μs, whereas Ce^{3+} shows considerably shorter decay times (some 60 ns in the wavelength range of interest). Another reason for saturation can be excited state absorption, i.e., a two-photon absorption process in which absorption, rather than emission from the excited state takes place. In many cases, the second excited state reached is the conduction band. This essentially corresponds to further oxidation of the activator ions. The most common activator ions in LEDs: Ce^{3+} and Eu^{2+} both also have a higher oxidation state (viz. Ce^{4+} and Eu^{3+}).
- High chemical- and photo stability, projected LED lifetimes are some 50.000–100.000 hours.

The requirement of strong absorption implies that activators are needed that show allowed optical transitions. Alternatively, sensitizers having allowed optical absorptions with emission spectra that show spectral overlap with the absorption spectra of activator ions are needed. The energy transfer concept is not as versatile as in fluorescent lamps, in view of the much smaller energy difference between absorption and emission in LED based lamps. Please note that energy transfer generally goes hand in hand with energy loss on the sensitizer and the activator ion.

Activators with allowed optical transitions in the near UV-VIS range are, e.g., Ce^{3+}, Eu^{2+} and Yb^{2+}, the emission time of the Yb^{2+} emission is very long (ms), for this reason there is not much focus on this ion. Mn^{4+} is also used, its optical transitions in the visible part of the spectrum are parity forbidden, the line emission of this ion (in the red!) is in addition spin-forbidden.

Both Ce^{3+} and Eu^{2+} enable allowed optical absorptions (of the 4f–5d) type. On the free ion (in vacuum) with no coordinating other ions, these transitions are located in the UV. By a combination of chemical bond tuning, reducing the charge density on the ligands (covalent bonds needed), and crystal

field interaction (the excited electron samples the symmetry of chemical environment leading to lifting of orbital degeneracy and is also sensitive to the charge of the coordinating ligands), these transitions can shifted into the visible part of the spectrum, see Figure 3 (for the Ce^{3+} ion as an example, but the principle holds for any 4f–5d transition) and Table 1. In case of Ce^{3+}, the ground state is split due to spin-orbit interaction. The inset in the left part of the figure shows the case of Ce^{3+} emitting in the UV. This requires a relatively small overall shift.

Table 1. Overview of some Ce^{3+} and Eu^{2+} phosphors showing the wide tunability range.

Luminescent material	Emission maximum (nm)
$LuPO_4$:Ce	316
$LaBr_3$:Ce	358
$Lu_2Si_2O_7$:Ce	380
Lu_2SiO_5:Ce	420
LuI_3:Ce	472
SrS:Ce	482
$Lu_3Al_5O_{12}$	520
$Y_3Al_5O_{12}$:Ce	550
SrB_4O_7:Eu	371
$Sr_2P_2O_7$:Eu	420
$BaMgAl_{10}O_{17}$:Eu	453
$SrAl_2O_4$:Eu	520
$CaGa_2S_4$	555
$Sr_2Si_5N_8$:Eu	620
CaS:Eu	650

The approach relies on the fact that the excited d-states are extended in space and for this reason are sensitive to the local environment. In the last two decades an impressive number of new compounds have been found, suitable for application in LED lamps. A disadvantage of Ce^{3+} and Eu^{2+} is that these ions in general show a large Stokes Shift, this being difference in energy between optical absorption and emission of the same optical transition (which is also due to the fact that de d-states are extended in space and participate in the chemical bonding in the excited state). This results in broad bands (FWHM typically larger than some 50–80 nm), on the other hand it prevents concentration quenching in view of the reduced spectral overlap between absorption- and emission bands. Especially in the red spectral range, broad bands are highly undesired, as argued above.

Interestingly, in case of Eu^{2+} an exceptional observation has been made that shows the principal possibility to get emission with a relatively small band width in combination with a relatively large Stokes Shift, in, e.g., $CsSr(P_2O_7)$:Eu [8, 9]. This effect is not completely understood, it very likely is related to asymmetric relaxation of the excited Eu^{2+} state, experimental proof is still lacking. Similar effects are also observed for ions with an s^2 electronic configuration in the ground state (like Bi^{3+} or Sb^{3+}) in phosphates, see [10, 11], where these effects have been interpreted in terms of a Jahn-Teller deformation in the excited state.

To deal with the need for narrow band red, the emission of Mn^{4+} has been revisited [12, 13]. Mn is a transition metal; the optical transitions used in LEDs are of the 3d-3d type and for this reason parity forbidden. The line emission on Mn^{4+} is also spin forbidden. The line emission of Mn^{4+} is located at relatively large wavelengths for lighting applications in systems known nowadays, see, f.e., Figure 4. In view of the fact that Mn^{4+} is a transition metal ion, it is fundamentally possible to shift the line emission, in contrast to the emission lines of rare-earth ions. Cr^{3+} has the same electronic configuration as $Mn^{4+}(d^3)$ and for this ion, the emission lines with the same physical origin are found at considerably

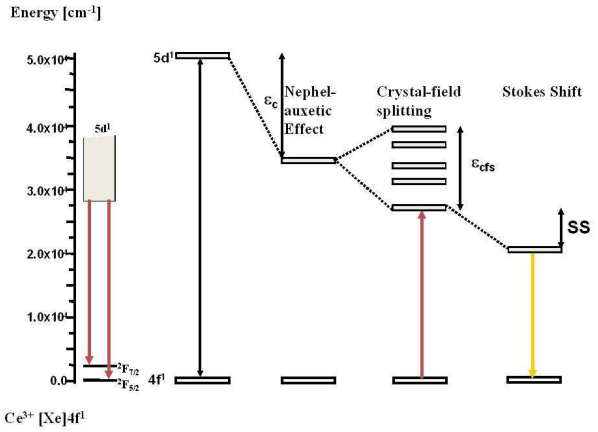

Figure 3. Strategies to tune the emission wavelength of Ce^{3+} containing luminescent materials.

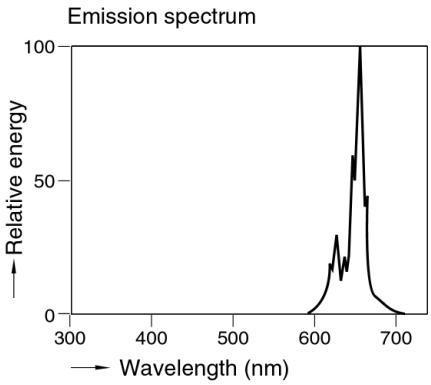

Figure 4. Mn^{4+} emission in $Mg_4GeO_{5.5}F$:Mn.

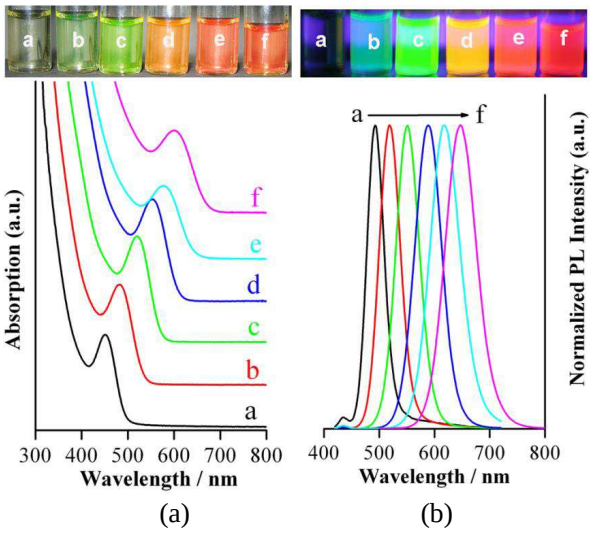

Figure 5. (a) Absorption and (b) emission spectra of CdTe quantum dots with different sizes, coated with mercaptosuccinic acid. (Figure is taken from [19]). The insets show (a) the daylight color and (b) the emission color, respectively.

longer wavelength, about 700 nm. Tuning the line emission of Mn^{4+} to even shorter wavelengths to make it more suitable for lighting applications can be achieved by making the chemical bond between Mn^{4+} and the surrounding ligands more ionic.

The luminescent materials used in LEDs can be applied as powder layers, and this is done frequently. Alternatively, also thin ceramic plates can be made. This has a number of advantages. First the heat conductivity of such ceramic plates is much better than of a powder layer, this is very advantageous in case of luminescent materials that tend to suffer from thermal quenching, a process in which the quantum yield decreases with increasing temperature. Secondly, LEDs tend to show small wavelength to wavelength variations, even when they originate from the same wafer. Also the small ceramic tiles have small variations in their optical properties. The ceramic plate concept allows binning: looking for LED die and ceramic tile combinations that strongly reduce LED to LED variation in the color of the light emitted. Philips applies this concept, which is called Lumiramic®.

In the search for narrow band red emission, quantum dots are investigated also. Quantum dots possess optical properties that are size dependent, both the absorption and the emission properties can

be tuned to a large extent for particles with sizes in the nm regime The emission bands of individual quantum dots are relatively narrow in view of a rather small energy difference the energetically lowest absorption band and the emission band (delocalized optical transitions, resulting in a very limited lattice relaxation). Rather narrow size distributions are required to obtain macroscopic amounts of quantum dots that possess narrow emission spectra (FWHM can be smaller than some 40 nm, see also Figure 5 for CdTe), and a lot of research and development attention goes into this direction, see, a.o., [14–20]. The feature of tunable line emission distinguishes quantum dots from line emitters based on rare-earth ions, where the spectral position of the lines only varies over a few nm (beit that many rare-earth ions show emission in many lines and that the relative intensities of these lines is host-lattice and in many cases also concentration dependent). The strong optical absorption, coupled to narrow band emission makes quantum dots almost ideal candidates for application in LEDs, provided that the quantum efficiencies are high enough. Application of coatings surrounding the quantum dots enables quantum efficiencies up to 90% and quantum dot based products have entered the market, see, e.g., [19]. In Figure 6, it is shown graphically how smaller spectral band width in the red part of the visible spectrum results in an increase of the amount of perceived light. The blue line represents the eye sensitivity curve under bright light conditions.

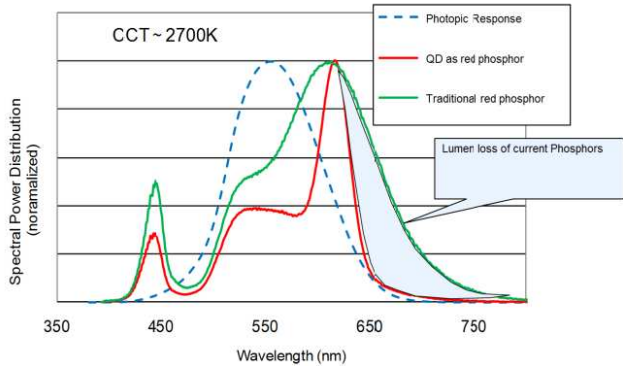

Figure 6. Emission spectrum of LEDs with a narrow band red emitter, showing increase of perceivable (red) light compared to LEDs with a traditional red emitting phosphor.

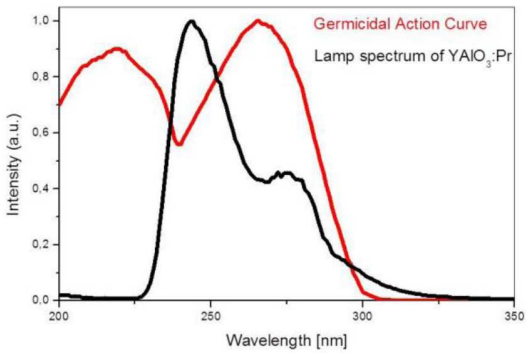

Figure 7. The spectral match of the emission spectrum of $YAlO_3$:Pr and the germicidal action curve.

2. LIGHT FOR DISINFECTION

The earth crust is covered to a large amount with water, yet the amount of sweet water is only a few percent, and of this few percent only a fraction is suitable for human consumption without further treatment. In many cases, surface water is contaminated by μ-organisms. UV radiation can be used to disinfect water, especially by preventing μ-organisms to reproduce, this being a consequence of photochemically induced cyclo-addition reactions between nucleotides on DNA. The disinfecting effect depends strongly on the wavelength, this is reflected in the so-called germicidal action curve (GAC), see Figure 7. This curve has maxima at about 220 nm and 270 nm.

There are several ways to generate UV radiation with the required wavelength:

- A low pressure Hg-discharge generates mainly UV photons with wavelength 254 nm, i.e., very useful radiation, without taking any extra measures like, f.e., using phosphors to down convert the radiation to the wavelength with optimum efficacy. This concept, however, has two disadvantages. Especially at lower temperatures, this kind of lamps has an outspoken run up behavior (Hg is a liquid at room temperature and needs to evaporate) which is a disadvantage in consumer applications and secondly there may be an uncontrolled release of Hg into the environment.
- Currently, there are worldwide investigations towards deep UV emitting LEDs in the material system (Al,Ga)N. This is a very promising concept, in view of the anticipated long life time

of LEDs and their low voltage operation. In addition, as they are approximately point light sources, they therefore also enable application of optical tools to adapt the final light distribution (etendue conservation). Further improvements, however, are needed in output power and cost-price reduction.

- Use of a Xe-discharge based radiation source. Please note that an important reason to use Xe is the fact that the VUV radiation is generated immediately after switching on this radiation source, as Xe is a gas at room temperature and does not need to evaporate to ensure proper lamp operation. The Xe-discharge generates mainly radiation in the VUV part of the optical spectrum, below 200 nm. This radiation is strongly absorbed by many media, also by water and even air. For this reason, the radiation generated by a Xe-discharge has to be downconverted to larger wavelength where both water and air show significantly less absorption. To this end, luminescent materials are needed that show a strong absorption at energies where the Xe-discharge emits and generate radiation preferably at the second maximum of the GAC curve. Main candidate activator ions for this kind of ions are Nd^{3+} and Pr^{3+}, showing emission due to optical transitions from the 5d to 4f states, similar to the cases of Eu^{2+} and Ce^{3+} treated above. In the conception of these luminescent materials, therefore, similar arguments are being used as in the conception of phosphors for LEDs, beit that the free ions have to have emission in the deep UV. Bi^{3+} can also be used, the optical transition on this ion is of a different kind, involving s- and p states, rather than f- and d states. Table 2 lists a number of materials that show desired optical properties. Figure 7 gives an example on the spectral match of the emission spectrum of YPO_4:Pr and the Germicidal Action Curve. Please note that that Bi is not a rare-earth ion.

Table 2. Luminescent materials for potential use in Xe-discharge based disinfection lamps.

Phosphor	Maximum emission wavelength (nm)
YPO_4:Nd	190
$LaPO_4$:Pr	225
YPO_4:Pr	233
YPO_4:Bi	241
YBP_2O_8:Pr	243
$CaSO_4$:Pr,Na	245
$YAlO_3$:Pr	245
$LuBO_3$:Pr	257
YBO_3:Pr	261
Lu_2SiO_5:Pr	265
Y_2SiO_5:Pr	270
$Lu_3ScAl_4O_{12}$:Bi	279

3. LIGHT FOR MEDICAL APPLICATIONS

Medical imaging is another important application for photonic materials. The so-called scintillating materials convert ionizing radiation used in, e.g., medical imaging into near UV or visible photons. These latter photons are, in turn, detected using photodiodes or photomultipliers. We first discuss two important imaging modalities, viz. Computed Tomography (CT) and Positron Emission Tomography (PET).

In CT, X-rays traverse through the patient and differences in X-ray absorption are being measured. As a consequence, anatomic images are created, based on differences in density. The X-ray source and

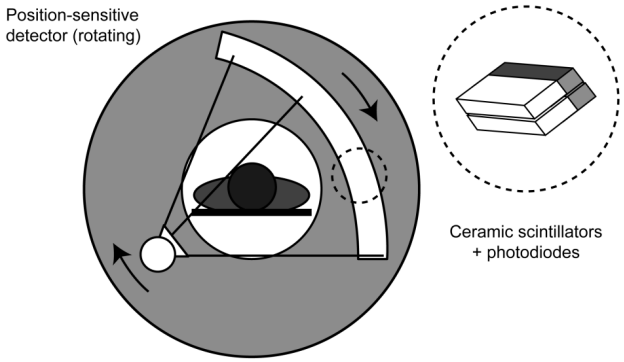

Figure 8. Principle of computed tomography. The X-ray source is located at the bottom, the scintillator array is depicted at the top of the figure. The anti-scatter grid is omitted for clarity reasons (figure taken from [21]).

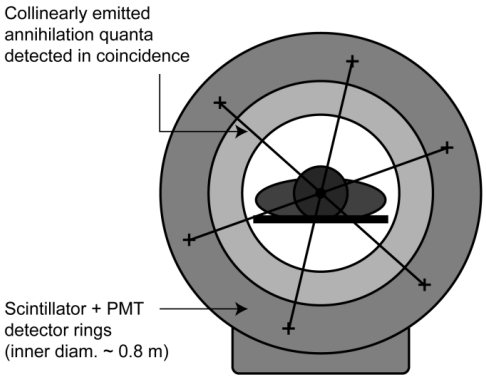

Figure 9. Principle of positron emission tomography instead of an external radiation source, a radioactive tracer emits gamma quanta inside the body of the patient. The scintillators are located in front of the detectors that form a ring around the patient. Also depicted is the line of response (figure taken from [21]).

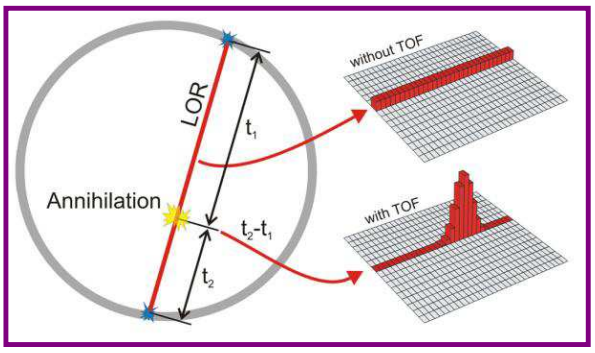

Figure 10. Principle of PET and time of flight PET. In case of TOF-PET, the difference in arrival time of two γ-quanta originating from the same annihilation event is measured as well.

the detection unit rotate around the patient, with a frequency up to a few Hertz, see also Figure 8. In this way, cross-sectional images of the body can be obtained from the data gathered.

In case of PET (Figures 9 and 10), the patient is injected with a radioactive material that emits positrons, i.e., there is no radiation source outside the patient's body. Positrons originating from the radioactive material and electrons stemming from the patient's body annihilate, resulting in two γ-quanta that are emitted under an angle of 180 degrees, this builds the Line of Response (LOR). Both γ-quanta have an energy corresponding to the rest mass of an electron, i.e., 511 keV. The straight line, building the LOR, and the identical γ-quanta photon energies follow from the requirement of the conservation of energy and momentum. The directions of the LORs are not governed by any conservation rule and consequently the γ-quanta pairs are emitted in opposite directions under all angles. Using reconstruction software, regions of interest are found. In case of a radioactive sugar, in this way regions in the body are indicated with a high metabolic activity, f.i., cancerous tissue. For this reason, PET is a considered a functional imaging modality.

To be able to derive the line of response, the two γ-quanta have to be detected in coincidence. In an even more advanced concept, the difference in arrival time of the two γ-quanta is measured (Time of Flight PET, TOF-PET). As a result reconstruction is easier since the spatial distribution of possible events is limited. This gives faster (statistical/iterative) reconstruction and less noise. This improves the signal to noise ratio, as noise origination from different locations can be discarded (Figure 10).

The scintillator material properties have a significant influence of the performance of PET and CT, see Table 3.

Table 3. Most important material properties and imaging parameters most strongly impacted by scintillators for CT and PET.

Imaging modality/Material property	Light yield	Decay time	Rise time	Afterglow	Stopping power
CT	Signal to noise ratio	Rotation speed	-	Rotation speed	Scintillator layer thickness
PET	Signal to noise ratio Coincidence timing Energy resolution	Coincidence timing Pile-up	Coincidence timing	When high too many non-coincident triggers	Spatial resolution Energy resolution

In CT, the light yield of the scintillators has to be as high as possible, the frequently used scintillator Gd_2O_2S:Pr has a light yield of some 40000 ph/MeV. The decay time of this material is small, viz. only 3.4 µs. Other materials also in use are $(Y,Gd)_2O_3$:Eu with a significantly larger decay time (1 ms) and a light yield of 19000 ph/MeV, see, e.g., [21]. Since a few years also garnet materials doped with Ce^{3+} are being used. Garnets show light yields up to 60000 ph/MeV and when doped with Ce^{3+} their primary decay time when excited with ionizing radiation is smaller than 100 ns, beit that in many cases longer decay components due to the presence of shallow traps and afterglow as a consequence of the presence of deep traps is observed. It is also observed that the luminescence properties and the light yield strongly depend on the material composition, see, f.e., [22–29]. Both $(Y,Gd)_2O_3$:Eu and the garnets are cubic, and transparent ceramic material can be obtained without the need for single crystal growth. This is a strong advantage in terms of manufacturing costs. In translucent materials, such as Gd_2O_2S:Pr, light scattering takes place, prolonging the optical pathway in the scintillator layer in a statistical manner. This, in turn, leads to statistical variations in the light output, f.e., due to optical self-absorption of the visible photons, and for this reason effectively in additional noise due to differences in signal gain. This can expressed in the so-called Swank factor, see [30].

Both a long decay time and afterglow would reduce the possible rotation speed in CT imaging procedures, prolonging the examination time and reducing the picture quality as the patients have to breathe during the procedure and may also move for different reasons. Especially the effects of a long decay time on the image quality can be diminished by appropriate mathematical algorithms. A high stopping power of the scintillating materials used in CT can reduce their thickness; this is rather advantageous in case of translucent materials, such as Gd_2O_2S:Pr. A high stopping power may also reduce material costs, in view of the thinner layers needed.

For PET, the light yield is important as well, especially for a high energy resolution. When a γ-quantum interacts with human tissue on its way to the detector by Compton scattering, it can lose or gain energy. This is coupled to a change in its direction. This change in direction would lead to an inaccurate LOR. The only way to detect this is by exactly measuring the energy of the γ-quantum that impinges on the scintillator. This corresponds to counting the number of photons generated. γ-quanta that generate too large or too small an amount of visible photons have to be rejected as their direction has changed during their trip to the detector. The spread in the number of photons generated by scintillators is quantified in their so-called energy resolution. The lower the value for the energy resolution, the better the photons that have Compton scattered can be discriminated from those that have not. Usually, the energy resolution is calculated using pulse height spectra.

As the number of photons at $t = 0$ is proportional to the light yield and inversely proportional to the decay time, for accurate coincidence timing, the light yield of scintillators for application in TOF-PET scintillators has to be as high and the decay time has to be as short as possible. When there is a buildup in the emission intensity (expressed as emission rise time), even when it is on the ns scale, for this reason the coincidence timing resolution will decrease. Fast energy transfer to the luminescent

ions is needed, on the sub ns time scale, to prevent such a build-up. The decay time has to be short as well in view of pile-up. When a γ-quantum hits a scintillator, the scintillator should not be excited a second time while the system is still counting the photons generated as a consequence of absorption of the first photon. When this happens, both events have to be rejected and both γ-quanta are lost.

To be able to use Si-based photomultipliers, the emission has to be located in the visible part of the spectrum. The combination of all effects discussed (visible emission, fast decay) renders Ce^{3+} as the only ion that can be used in this kind of scintillators. The emission wavelength of this ion is tuned into the desired spectral range using the strategy developed above (for application in LEDs and in light sources for disinfection). In view of the large photon energy (511 keV), crystals are needed with length in the order of a few cm to absorb the energy of the γ-quanta completely (high stopping power). This, in turn, requires the material to be transparent, to prevent photon losses due to scattering in the material. In current TOF-PET machines $(Lu,Y)_2SiO_5$:Ce is being used, this material has a light yield of about 40000 photons/MeV and a decay time of about 40 ns. Especially the large amount of Lu, together with the need to grow single crystals, makes this material very expensive. A potential way out is the use of cubic materials that can be sintered to transparency, this strongly reduces processing costs. The cubic garnet type of materials doped with Ce^{3+}, also used in LEDs, are potentially suitable for application in (TOF)-PET and to this end are investigated by many different groups, both in academia and companies, see, a.o., [22–29]. In comparison with $(Lu,Y)_2SiO_5$:Ce, their light yield is high, but especially their decay time is large and in addition contains long decay components, due to trapping. Their Figure of Merit (FoM) (Light yield/decay time) is smaller than that of $(Lu,Y)_2SiO_5$:Ce. Interestingly, the decay time of the garnets when excited with UV light is in the order of 60 ns. When trapping effects would not play a role, garnets would have the same FoM as $(Lu,Y)_2SiO_5$:Ce. This underlines the importance of understanding the energy flow in scintillating materials.

Afterglow will lead to additional triggering of the PET counting system, without the detection of two simultaneously generated γ-quanta. The stopping power is also important for the spatial resolution of TOF-PET. When the γ-quanta do not hit the scintillator elements parallel to their length axis, the probability that they deposit (part of) their energy in a next scintillator element (pixel) increases (Depth of Interaction effect).

Finally, when the lattice density of the scintillators is high, non-linear effects, deteriorating the energy resolution become important. The absorption of ionizing radiation leads to the creation of fast electrons and (core) holes. These highly excited particles further thermalize by Auger processes and fluorescence (creating photons with high energies) due to transitions involving core levels. The energy transfer to the lattice increases with decreasing kinetic energy of the electrons. Eventually electron hole pairs over the band gap and also excitons may be formed. Interaction between these excited (quasi) particles, f.e., again due to Auger processes between charge carriers in the valence and conduction band, will result in energy loss. The probability of such processes to occur increases more than linearly with the density of these particles. Therefore, fast diffusion of charge carriers or excitons is needed to reduce the density of charge carriers and/or excitons out of the regions with a high density of electron-hole pairs across the band gap and/or excitons. Energy transfer will also lead to energy diffusion. In materials with a high stopping power, the density of excited particles is larger than in low density materials, this is expected to deteriorate the energy resolution in materials with a high density as the stopping power increases more than linearly with the density [21]. The mobility of the excited particles decreases with increasing refractive index due to trapping effects, also for this reason host materials with a high stopping power (with higher electron densities and therefore a larger refractive index) are expected to show worse energy resolution, see, e.g., [31] for a broad overview. Variations in the lattice potential are also expected to reduce the mobility of the excited particles. Interestingly, there is much focus on garnets containing a lot of different metal ions, as this improves the overall energy efficiency, see, e.g., [22–29], this may come with a compromise in terms of energy resolution.

4. LIGHT FOR HORTICULTURE

The last section of this paper deals with light for horticulture. The rapid growth of the earth's population requires efficient means to produce food with a high nutritional value. Green houses are used for a long time already, the advent of LEDs has opened up the possibility to create optimized and tailored light

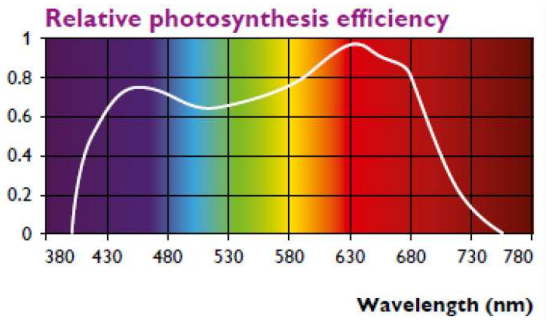

Figure 11. Relative photosynthesis efficiency as function of the wavelength.

created with a very high efficiency. In addition, due to their very nature, heat and light can be coupled out into different directions. In more traditional light sources, a higher light intensity results in heating the plants considerably, this sets a limit to the light intensity that could be used. LED light sources do, if at all, hardly suffer from this effect.

In Figure 11, the relative photosynthesis efficiency is given as a function of the wavelength. We observe the highest efficiency at the short wavelength- and the long wavelength side of the visible light spectrum, at locations where the eye sensitivity is rather low. We also observe a high efficiency at the spectral position where low pressure Na-lamps have their emission maximum (590 nm). Application of LEDs in horticulture therefore requires dedicated light sources for optimal efficiency. This can be done by a combination of LEDs, f.e., LEDs emitting in the deep blue and emitting in the far red. Additional LEDs, emitting at different wavelengths, can be added as well. Other solutions rely on blue light emitting LEDs, in which part of the light is converted into deep red light, essentially the same concept as white light emitting LEDs based on down conversion by luminescent materials. As the requirements to be fulfilled by these devices differ considerably from the requirements to be fulfilled by efficient light sources, new luminescent materials would have to be developed in this concept, showing emission in the deep red part of the spectrum, Eu^{2+} phosphors could be used in rather covalent host lattices, beit that at too low wavelengths, thermal quenching may happen, due to crossing of the parabola describing ground- and excited states near to the relaxed excited state. Alternatively also transition metal ions like $Cr^{3+}(d^3)$, Mn^{2+} (d^5) or $Mn^{4+}(d^3)$ could be used. In case of Cr^{3+}, dependent on the local coordination of the Cr^{3+} ion, both broad bands and line emission (at about 700 nm) can be obtained. To obtain line emission, the crystal field acting on the Cr^{3+} should be strong, otherwise broad band emission is obtained that, dependent on the crystal field strength, can be located in the spectral region of interest. In case of Mn^{4+}, the crystal field is always that strong that line emission (in known systems at wavelengths above 600 nm) is obtained. Some materials, emitting in the spectra region of interest, are given in Table 4, beit this list is far from complete. For the transition metal ions, the optical transitions are at least parity forbidden; this may imply the use of ceramic tiles, like in the Lumiramic® concept. In case of strongly absorbing materials, also remote systems can be used, with indirect illumination of the luminescent materials.

Table 4. Some luminescent materials showing deep red emission.

Material	Emission maximum (nm)
$GdMgB_5O_{10}$:Mn (Mn^{2+})	630
CaS:Eu	645
CaS:Eu, Mn (Mn^{2+})	657
$Mg_4GeO_{5.5}F$:Mn (Mn^{4+})	660 (several peaks)
Al_2O_3:Cr	694 (several peaks)
$Y_3Al_5O_{12}$:Cr	710 (several peaks)

Eventually Lighting Recipes can be developed, indicating the light level, the spectrum, the required uniformity the light source position and the illumination time needed. It also indicates the parameters for which the recipe is valid, e.g., the climate conditions. Finally, it indicates the results to be expected beyond energy savings, see also [32].

5. SUMMARY

An overview has been given indicating the very intimate relationship between device development and the underlying materials science. Using examples from a number of different application areas, it has been shown how materials science can be used to significantly improve the performance of devices based on the performance of luminescent materials.

ACKNOWLEDGMENT

The author thanks Prof. Thomas Juestel, (University of Applied Sciences, Muenster, Germany) and Dr. Rolf Koole, Dr. Sjoerd Mentink and Dr. Herfried Wieczorek (Philips Research, Eindhoven, the Netherlands) for useful comments and some of the pictures.

REFERENCES

1. Meyer, F., H. Spanner, and E. Germer, "Metal vapor lamp," US Patent 2.182.732, 1927.
2. Inman, G., "Electric discharge lamp," US Patent 2.259.040, 1936.
3. http://en.wikipedia.org/wiki/CIE_1931_color_space.
4. Sommerdijk, J. L., A. Bril, and A. W. de Jager, "Two photon luminescence with ultraviolet excitation of trivalent praseodymium," *J. Lum.*, Vol. 8, 341, 1974.
5. Piper, W. W., J. A. de Luca, and F. S. Ham, "Cascade fluorescent decay in Pr^{3+}-doped fluorides: Achievement of a quantum yield greater than unity for emission of visible light," *J. Lum.*, Vol. 8, 344, 1974.
6. Wegh, R. T., H. Donker, K. D. Oskam, and A. Meijerink, "Visible quantum cutting in $LiGdF_4$:Eu^{3+} through downconversion," *Science*, Vol. 288, 663–666, 1999.
7. Oskam, K. D., R. T. Wegh, H. Donker, E. V. D. van Loef, and A. Meijerink, "Downconversion: A new route to visible quantum cutting," *Journal Alloys and Compounds*, Vol. 421, 300–301, 2000.
8. Srivastava, A. M., H. A. Comanzo, S. Camardello, M. Aycibin, and U. Happek, "Luminescence of octahedrally coordinated Eu^{2+} in $Rb_2MP_2O_7$ (M = Ca, Sr)," *ECS Transactions*, Vol. 25, 201, 2009.
9. Srivastava, A. M., H. A. Comanzo, S. Camardello, S. B. Chaney, M. Aycibin, and U. Happek, "Unusual luminescence of octahedrally coordinated divalent europium ion in $Cs_2M^{2+}P_2O_7$ (M^{2+} = Ca, Sr)," *J. Lumin.*, Vol. 129, 919, 2009.
10. Oomen, E. W. J. L., W. M. A. Smit, and G. Blasse, "Jahn-Teller effect in the emission and excitation spectra of the Sb^{3+} ion in LPO_4 (L = Sc, Lu, Y)," *Phys. Rev. B*, Vol. 37, 18, 1988.
11. Oomen, E. W. J. L., W. M. A. Smit, and G. Blasse, "Luminescence of the Sb^{3+} ion in calcium fluorapatite and other phosphates," *Mat. Chem. and Phys.*, Vol. 19, No. 4, 357, 1988.
12. Setlur, A. A., E. V. Radkov, C. S. Henderson, J.-H. Her, A. M. Srivastava, N. Karkada, M. Satya Kishore, N. Prasanth Kumar, D. Aesram, A. Deshpande, B. Kolodin, L. S. Grigorov, and U. Happek, "Energy-efficient, high-color-rendering LED lamps using oxyfluoride and fluoride phosphors," *Chem. Mat.*, Vol. 22, No. 13, 4076, 2010.
13. Radkov, E. V., L. S. Grigorov, A. A. Setlur, and A. M. Srivastava, "Light emitting diodes; semiconductor light source coupled to a complex fluoride phosphor-activated with Mn^{4+}," US Patent 7497973 B2, 2009.
14. Shirasaki, Y., G. J. Supran, M. G. Bawendi, and V. Bulović, "Emergence of colloidal quantum-dot light-emitting technologies," *Nature Photonics*, Vol. 7, 13, 2013.

15. Shen, H., S. Wang, H. Wang, J. Niu, L. Qian, Y. Yang, A. Titov, J. Hyvonen, Y. Zheng, and L. S. Li, "Highly efficient Blue-Green quantum dot light-emitting diodes using stable low-cadmium quaternary-alloy ZnCdSSe/ZnS core/shell nanocrystals," *ACS Appl. Mater. Interfaces*, Vol. 5, No. 10, 4260, 2013.
16. Coe-Sullivan, S., "Optoelectronics: Quantum dot developments," *Nature Photonics*, Vol. 3, 315, 2009.
17. Sun, Q., Y. A. Wang, L. S. Li, D. Wang, T. Zhu, J. Xu, C. Yang, and Y. Li, "Bright, multicoloured light-emitting diodes based on quantum dots," *Nature Photonics*, Vol. 1, 717, 2007.
18. Qu, L. and X. Peng, "Control of photoluminescence properties of CdSe nanocrystals in growth," *J. Am. Chem. Soc.*, Vol. 124, No. 9, 2049, 2002.
19. http://www.qdvision.com/.
20. Ying, E., D. Li, S. Guo, S. Dong, and J. Wang, "Synthesis and bio-imaging application of highly luminescent mercaptosuccinic acid-coated CdTe nanocrystals," *PLoS ONE*, Vol. 3, No. 5, e2222, doi:10.1371/journal.pone.0002222, 2008.
21. Ronda, C. R. and A. M. Srivastava, *Luminescence: From Theory to Applications*, Chapter 5, edited by C. R. Ronda, VCH Weinheim, Germany, 2007, ISBN: 978-3-527-31402-7.
22. Babin, V., M. Nikl, K. Kamada, A. Beitlerova, and A. Yoshikawa, "Effect of the $Pr^{3+} \longrightarrow Gd^{3+}$ energy transfer in multicomponent garnet single crystal scintillators," *J. Phys. D: Appl. Phys.*, Vol. 46, 365303, 2013.
23. Kamada, K., T. Yanagida, J. Pejchal, M. Nikl, T. Endo, K. Tsutsumi, Y. Usuki, Y. Fujimoto, A. Fukabori, and A. Yoshikawa, "Scintillation properties of Ce doped $Gd_2Lu_1(Ga,Al)_5O_{12}$ single crystal grown by the micro-pulling-down method," *Journal of Crystal Growth*, Vol. 352, 35, 2012.
24. Kamada, K., T. Yanagida, J. Pejchal, M. Nikl, T. Endo, K. Tsutumi, Y. Fujimoto, A. Fukabori, and A. Yoshikawa, "Scintillator-oriented combinatorial search in Ce-doped $(Y,Gd)_3(Ga,Al)_5O_{12}$ multicomponent garnet compounds," *J. Phys. D: Appl. Phys.*, Vol. 44, 505104, 2011.
25. Ogiegło, J. M., A. Katelnikovas, A. Zych, T. Juestel, A. Meijerink, and C. R. Ronda, "Luminescence and luminescence quenching in $Gd_3(Ga,Al)_5O_{12}$ Scintillators doped with Ce^{3+}," *J. Phys. Chem. A*, Vol. 117, 2479, 2013.
26. Ogiegło, J. M., A. Zych, T. Juestel, A. Meijerink, and C. R. Ronda, "Luminescence and energy transfer in $Lu_3Al_5O_{12}$ scintillators co-doped with Ce^{3+} and Pr^{3+}," *Optical Materials*, Vol. 35, 322, 2013.
27. Ivanovskikh, K. V., J. M. Ogiegło, A. Zych, C. R. Ronda, and A. Meijerink, "Luminescence temperature quenching for Ce^{3+} and Pr^{3+} d-f emission in YAG and LuAG," *ECS J. Solid State Science and Technology*, Vol. 2, R3148, 2013.
28. Ogiegło, J. M., A. Zych, K. V. Ivanovskikh, T. Juestel, C. R. Ronda, and A. Meijerink, "Luminescence and energy transfer in $Lu_3Al_5O_{12}$ scintillators co-doped with Ce^{3+} and Tb^{3+}," *J. of Phys. Chem. A*, Vol. 116, 8464, 2012.
29. Ivanovskikh, K. V., A. Meijerink, F. Piccinelli, A. Speghini, C. R. Ronda, and M. Bettinelli, "VUV spectroscopy of $Ca_3Sc_2Si_3O_{12}$:Pr^{3+}: Scintillator optimization by co-doping with Mg^{2+}," *ECS Journal of Solid State Science and Technology*, Vol. 1, R127, 2012.
30. Swank, R. K., "Absorption and noise in x-ray phosphors," *J. Appl. Phys.*, Vol. 44, 4199, 1973.
31. Khodyuk, I. V., "Nonproportionality of inorganic scintillators," Thesis, TU Delft, the Netherlands, 2013, ISBN: 978-90-8891-553-6.
32. http://www.lighting.philips.com/pwc_li/main/shared/assets/downloads/pdf/horticulture/leaflets/general-booklet-philips-led-lighting-in-horticulture-EU.pdf.